MRI-informed functional EIT lung imaging

J. L. Davidson[1], R. A. Little[2] P. Wright[1], M. Crabb[3], J. Naish[2], A. Morgan[2],
G. J. M. Parker[2], W. R. B. Lionheart[3], R. Kikinis[4] and H. McCann[1]

[1] School of Electrical and Electronic Engineering, University of Manchester, Manchester, UK
[2] Imaging Sciences, Biomedical Imaging Institute, University of Manchester, Manchester, UK
[3] School of Mathematics, University of Manchester, UK
[4] Surgical Planning Laboratory, Brigham and Women's Hospital, Harvard Medical School, Boston, USA

Email: j.davidson-2@manchester.ac.uk

Abstract **This paper gives illustrative results from a recent pilot study of functional dynamics of the lung with healthy male volunteers at the University of Manchester. 3D EIT reconstructions and MRI scans of basic lung function have been acquired in order to compare the two modalities. The outer surface of the MRI image of the torso, and electrode-positions obtained from MRI fiducial markers, aided the construction of a finite element model extruded along the long axis of the subject. Both EIT and MRI image data streams were co-registered using the open source medical imaging software, *3D Slicer*. The resultant data fusion provides a highly effective method of directly comparing EIT and MRI images. The EIT images show very good spatial resolution under dynamic conditions, revealing spatial and temporal differences in lung ventilation between the subject in the seated and supine positions.**

Introduction

Electrical Impedance Tomography (EIT) provides non-invasive, high temporal resolution functional imaging of the lung. However, EIT lacks the excellent spatial resolution of Magnetic Resonance Imaging (MRI), which is often a crucial requirement in fully understanding lung functionality or the progression of lung disease, e.g. chronic breathing disorders such as COPD (Chronic Obstructive Pulmonary Disorder). The inescapable conclusion is that with present technologies, the optimum combination of anatomical and functional imaging requires characterisation with more than one imaging modality. The overall aims of this present study are to provide an assessment of EIT spatial resolution compared with high resolution MRI, and to explore the fusion of the two modalities.

Experimental methods

Equidistantly spaced electrodes were arranged in two transverse rings of 16 on the chest at approximately the fourth and sixth intercostal spaces along with an abdominal reference electrode. EIT measurements were acquired using the EIT sub-system of the bio-medical fEITER instrument [1], a BS EN 60601-1:2006 compliant system which operates at 100 fps with SNR approaching 80 dB. In this study, a nearest-neighbour current injection protocol was used with a total of 20 current patterns which included 8 independent horizontal injections per electrode ring. All current injections were 1 mA pk-pk at 10 kHz and the EIT instrument recorded nearest-neighbour voltage pairs at 100 frames per second (fps). EIT data were recorded whilst the subject carried out basic breathing procedures in 1 minute blocks. Breathing procedures involved normal and progressively deeper tidal breathing regimes interspaced with reference conditions of typically 5-second breath-holds at both inspiration and expiration. MRI fiducial markers were placed on the subject at all EIT electrode locations immediately after the last EIT data collection, before carrying out MRI scanning using a T2-weighted HASTE protocol on a 1.5 T Philips Achieva. MRI scans were performed under the same breathing procedures as used during the EIT tests. MRI scans included ten 1 cm contiguous axial slices which were cardiac gated and acquired for the conditions of normal breath-holding and at maximum inspiration and expiration.

Typical raw EIT measurements

Figure 1(a) shows typical voltage measurement data for two measurement sites; site 1 refers to voltages at an anterior Right-Hand-Side (RHS) location on the upper electrode ring, whilst site 2 refers to a posterior Left-Hand-Side (LHS) location on the lower electrode ring. The periodic sinusoidal nature of the data is consistent with the breathing rate of the subject. Additionally, the significant differences in the 'phase' of the voltage changes for the two different sites suggests spatial differences of the underlying conductivity distribution within the lung. More complicated patterns of measured data have been observed for sites in close proximity to the heart as shown in Figure 1(b) which exhibits higher frequency components related to heart rate. Such observations illustrate the excellent low noise characteristics (< 6 μV rms) of raw human data from the fEITER EIT sub-system at 100 fps.

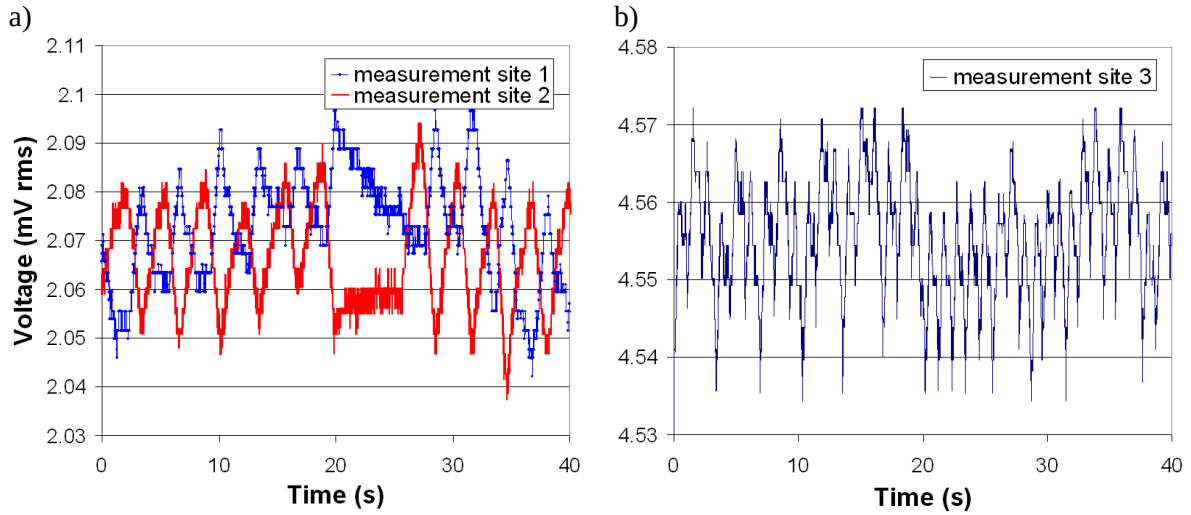

Figure 1. Typical voltage measurements for a seated subject whilst performing shallow breathing; (a) two different measurement sites involving a 5-second breath-hold (at inspiration) at 20 seconds and (b) measurement site over the heart showing cardiac related changes.

Image reconstruction

The external boundary shape of the subject was obtained from a selected MRI transverse image slice chosen at a mid-plane between the two electrode rings. Typically, the contour of this shape was defined by approximately 50 points which were used to produce a 3D finite element model extruded along the long axis of the subject. The approximation to body shape was performed using the EIDORS [2] in-built *ng_mk_extruded_model* function calling the Netgen mesh generator [3]. The method has been applied to swine data and described by Grychtol *et al* [4]. Figure 2 shows typical EIDORS difference image reconstructions using a one-step linearised Gauss-Newton method with standard Tikhonov regularisation.

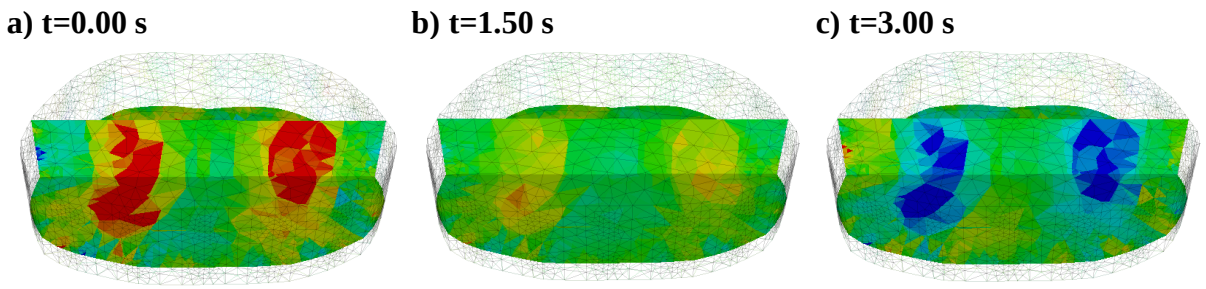

Figure 2. 3D reconstructions rendered in MayaVi software [5] during a breathing cycle showing conductivity changes during inhalation and exhalation. Transverse and coronal scalar-cut planes are shown within the 3D volume (front of chest in the background).

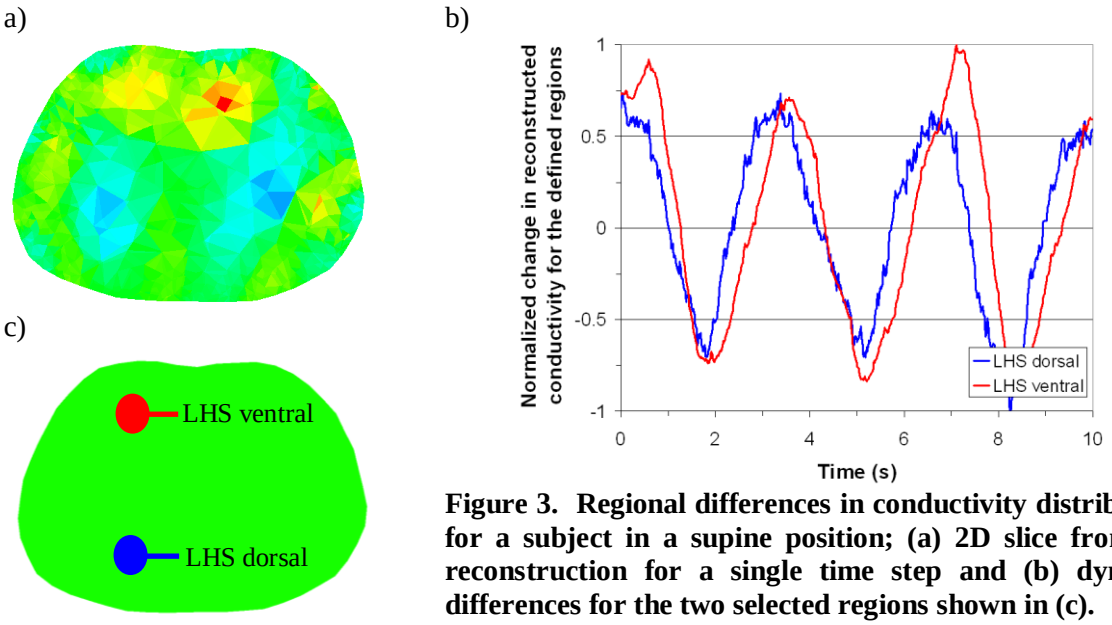

Figure 3. Regional differences in conductivity distribution for a subject in a supine position; (a) 2D slice from the reconstruction for a single time step and (b) dynamic differences for the two selected regions shown in (c).

Figure 3(a) shows a 2D slice from an EIDORS 3D image reconstruction at a single time step for a subject in the supine position whilst performing moderate tidal breathing. Regional differences in the conductivity distribution can be clearly seen due to gravitational effects on the subject as described by Frerichs *et al* [6 and 7]. In this case, the dynamic behaviour is illustrated in Figure 3(b) for averaged solution data within a 15 mm search radius for the regions shown schematically in Figure 3(c). Temporal and amplitude differences in the regional traces can be clearly seen in a consistent manner over successive breathing cycles.

Data fusion example

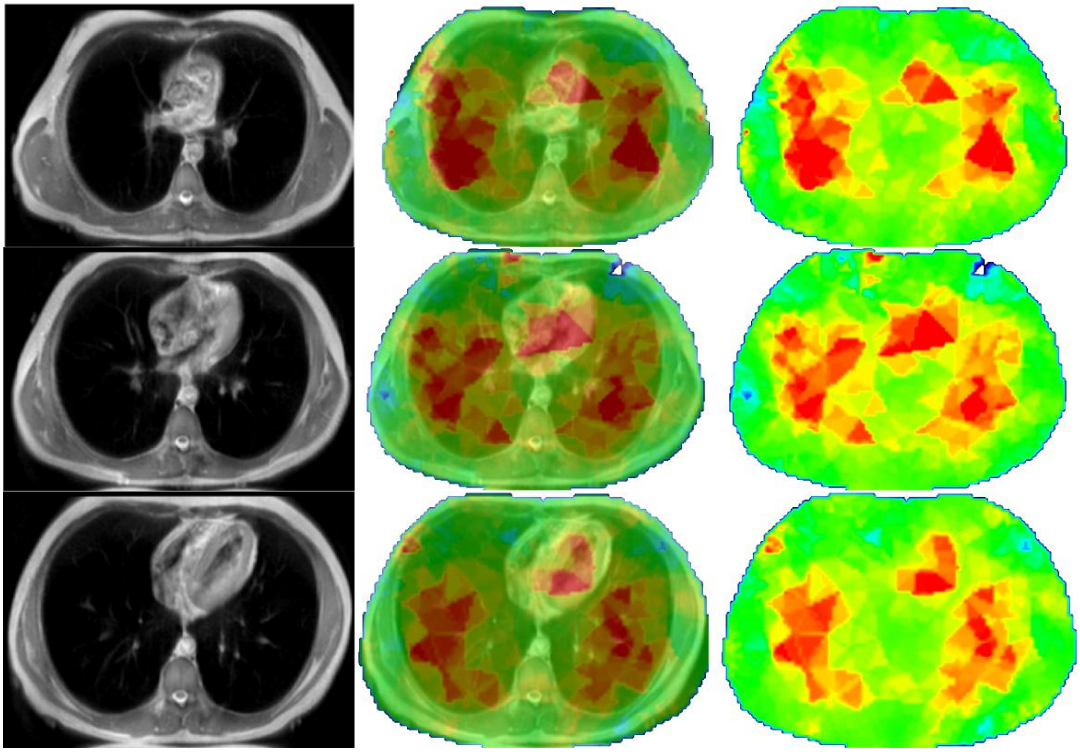

Figure 4. Data fusion example using *3D Slicer* software. Top to bottom: superior to inferior views for MRI image at maximum inspiration (far LHS), fused EIT/MRI image (middle) and EIT difference image (far RHS).

The Manchester *Confeitir* [8] software package was used to convert the reconstructed EIT data from the irregular tetrahedral mesh into a matrix with 2 mm-cubic isotropic voxels each representing a conductivity change. The output of *Confeitir* is a format which is consistent with MRI data structures. The method has been validated [9] with bench-top phantoms and reported at EIT 2011. Both the MRI and EIT data were imported into the open source visualization and analysis software *3D Slicer* [10]. Manual translation and rotations were applied until they were visually aligned, aided by the position of the MRI fiducial markers in relation to the EIT electrode locations clearly visible from the increased mesh density within the model. Figure 4 shows examples of the resulting transverse images from the two data sets. A visual inspection of these images suggests good correspondence between the two modalities.

Conclusions and future work

Our initial data demonstrate high SNR, high temporal resolution MRI-informed EIT reconstructions of human lung function. The data fusion process provides a highly effective method of directly comparing EIT images with those obtained from MRI. Further data analysis will enable a more systematic and quantitative determination of EIT spatial fidelity. Future work will also include a comparison of the sensitivity of EIT measurements across a range of subject-specific models.

Acknowledgements

This work is funded via the RCUK Science Bridges award, EPSRC Ref: EP/G041733/1. All EIT and MRI data collections were performed at the Wolfson Molecular Imaging Centre (WMIC) of the University of Manchester.

References

[1] McCann H, Ahsan S T, Davidson J L, Robinson R L, Wright P, and Pomfrett C J D (2011), A portable instrument for high-speed brain function imaging: fEITER, Proc. *33rd Annual Int. Conf. IEEE EMBS* (Boston MA, USA) pp. 7029-7032, DOI: 10.1109/IEMBS.2011.6091777

[2] Adler A and Lionheart W R B 2006 Uses and abuses of EIDORS: an extensible software base for EIT *Physiol. Meas.* **27** S25-42

[3] Schöberl J (1997) NETGEN – An advancing front 2D/3D-mesh generator based on abstract rules *Comput. Visual Sci.* **1** 41-52 (http://www.hpfem.jku.at)

[4] Grychtol B, Lionheart W R B, Wolf G K, Bodenstein M and Adler A (2011) The importance of shape: thorax models for GREIT, *Proc. 12th International Conference on Electrical Impedance Tomography* (Bath, UK)

[5] MayaVi scientific data visualizer at http://mayavi.sourceforge.net

[6] Frerichs I, Bodenstein M, Dudykevych T, Hinz J, Hahn G and Hellige G (2005) Effect of lower body negative pressure and gravity on regional lung ventilation determined by EIT *Physiol. Meas.* **26** S27-S37

[7] Frerichs I, Hahn G and Hellige G (1996) Gravity-dependent phenomena in lung ventilation determined by functional EIT *Physiol. Meas.* **17** A149-A157

[8] McCormick D, Davidson J L and McCann H (2007) Conversion of EIT brain images for co-registration in Proc. *13th International Conference on Electrical Bioimpedance and the 8th Conference on Electrical* (Graz, Austria) pp 384-387, ISBN 978-3-540-36839-7

[9] Davidson J L, Little R A, Wright P, Naish J, Kikinis R, Parker G J M and McCann, Fusion of images obtained from EIT and MRI *Electronics Letters* (submitted, 2012)

[10] Pieper S, Halle M and Kikinis R (2004) 3D SLICER in Proc. *1st IEEE International Symposium on Biomedical Imaging: From Nano to Macro* **1** 632-635 (see http://www.slicer.org)